frontiers in Marine Science

ORIGINAL RESEARCH
published: 20 April 2018
doi: 10.3389/fmars.2018.00130

ALOHA From the Edge: Reconciling Three Decades of *in Situ* Eulerian Observations and Geographic Variability in the North Pacific Subtropical Gyre

Maria T. Kavanaugh[1]*, *Matthew J. Church*[2], *Curtiss O. Davis*[1], *David M. Karl*[3], *Ricardo M. Letelier*[1] and *Scott C. Doney*[4]

[1] College of Earth, Ocean and Atmospheric Sciences, Oregon State University, Corvallis, OR, United States, [2] Flathead Lake Biological Station, University of Montana, Polson, MT, United States, [3] Daniel K. Inouye Center for Microbial Oceanography: Research and Education (C-MORE), University of Hawaii at Manoa, Honolulu, HI, United States, [4] Department of Environmental Sciences, University of Virginia, Charlottesville, VA, United States

OPEN ACCESS

Edited by:
Alison Buchan,
University of Tennessee, Knoxville,
United States

Reviewed by:
Jeffrey Polovina,
National Oceanic and Atmospheric Administration (NOAA), United States
Andrew Irwin,
Mount Allison University, Canada

***Correspondence:**
Maria T. Kavanaugh
mkavanau@ceoas.oregonstate.edu

Specialty section:
This article was submitted to Aquatic Microbiology, a section of the journal Frontiers in Marine Science

Received: 06 December 2017
Accepted: 28 March 2018
Published: 20 April 2018

Citation:
Kavanaugh MT, Church MJ, Davis CO, Karl DM, Letelier RM and Doney SC (2018) ALOHA From the Edge: Reconciling Three Decades of in Situ Eulerian Observations and Geographic Variability in the North Pacific Subtropical Gyre. Front. Mar. Sci. 5:130. doi: 10.3389/fmars.2018.00130

Global analyses of satellite and modeled data suggest decreased phytoplankton abundance and primary productivity in oligotrophic gyres as they expand in response to increased surface temperatures, shoaling of surface mixed layers, and decreased supply of subsurface macronutrients. However, analogous changes in the phytoplankton have not been evident *in situ* at Hawaii Ocean Time-series (HOT) Station ALOHA (22°45′N, 158°00′W), suggesting that physiological or structural reorganization not observed from space, uncorrected sensor drift, or uncharacterized geographic variability may be responsible for the apparent discrepancy. To address the latter, we compared interannual patterns of *in situ* phytoplankton dynamics and mixed layer properties to gyre extent and boundary location based on multiple definitions including dynamic topography, a threshold of satellite surface chlorophyll (chl *a*) $\leq$0.07 mg m^{-3}, and multivariate biophysical seascapes using modeled or satellite data. Secular increases in gyre extent were apparent, although the rate of expansion was much slower than previously reported, whereas strong interannual oscillations were evident for all definitions of the gyre. Modeled and satellite-based multivariate seascapes agreed well in terms of expansion (surface area of seascapes) and isolation of Station ALOHA (distance to seascape boundary) resulting in a combined data record of nearly three decades. Isolation was associated positively with the North Pacific Gyre Oscillation (NPGO), and negatively with Multivariate ENSO Index (MEI), and Pacific Decadal Oscillation (PDO). The converse was true for the gyre's expansion. Expansion followed a shoaling and freshening of the surface mixed layer and declines of *in situ* net primary production (PP) suggesting that Station ALOHA may serve as an early indicator of gyre biogeographic patterns. Lags between geographic indicators and *in situ* conditions appear to partially explain past observed discrepancies between patterns from satellite remote sensing and those from *in situ* conditions at Station ALOHA.

Keywords: climate oscillations, North Pacific Subtropical Gyre, dynamic geography, seascape ecology, Station ALOHA

INTRODUCTION

Covering over 20 million square kilometers, the North Pacific Subtropical Gyre (NPSG) is the largest ecosystem on the planet surface (Sverdrup et al., 1942; Karl, 2010). The permanently stratified surface layer in this system restricts the vertical fluxes of inorganic nutrients into the well-lit surface region, resulting in low primary production (PP) and export of carbon to the deep ocean. However, because of their size, open ocean regions like the NPSG are responsible for substantial oceanic primary and export production (Martin et al., 1987; Emerson et al., 1997). The debate is ongoing, however, as to how these processes are changing in response to longer term shifts in environmental forcing such as changes in ocean chemistry (Dore et al., 2009) and temperature (Karl et al., 2001; Corno et al., 2007; Saba et al., 2010). Accurate estimation of global ocean production and export, therefore, will require not only reliable estimation of NPSG ecosystem processes (Karl, 2010) but also a detailed understanding of the oceanographic context in which these processes are occurring, including an accurate characterization of gyre geography and the dynamics of gyre areal extent and boundary location.

Because of their immense size and age, oligotrophic gyres have been considered historically to support pelagic ecosystems in a climax state relatively resulting from stable environmental forcing in space and time; however, they are now recognized to display substantial spatial, seasonal, and interannual variability (Venrick, 1995; Karl, 2010; Karl and Church, 2017). While dominated by small phytoplankton and regenerated productivity (Letelier et al., 1996; Li et al., 2011), relatively short-lived perturbations in the NPSG contribute not only to momentary increases in net primary productivity (NPP) but also to the decoupling of autotrophic and heterotrophic processes and subsequent export of particulate carbon. These include deep vertical mixing events followed by water column restratification (DiTullio and Laws, 1991) associated with the passage of cyclonic eddies (Letelier et al., 2000; Wilson and Adamec, 2001), Rossby waves (Sakamoto et al., 2004), and the breaking of internal waves. On longer time scales, *in situ* PP and phytoplankton biomass (as determined by chlorophyll chl *a*) in the NPSG, measured during various programs such as CLIMAX and the Hawaii Ocean Time-series (HOT) have increased over the past four decades (Venrick et al., 1987; Karl et al., 2001; Corno et al., 2007). These increases have been linked to a shift in the phase of the Pacific Decadal Oscillation (PDO, Karl et al., 2001) or El Niño Southern Oscillation (ENSO)/PDO interactions (Corno et al., 2007) and resulting changes in stratification.

Station ALOHA (22.75°N, 158°W: A Long-term Oligotrophic Habitat Assessment) is a benchmark monitoring site in the NPSG where *in situ* sampling of ocean physical, biological, and chemical parameters has occurred since 1988 (Karl, 2010). However, the patterns of increased biomass and primary productivity found *in situ* are contrary to synoptic patterns observed through analyses of derived satellite products. Behrenfeld et al. (2006) observed that global ocean net PP and phytoplankton biomass (as defined by chl *a*) decreased from 1999 to 2006 in response to increased water column stratification. Hypothesized as an ecological response to an increase in the multivariate ENSO index, the chl *a* trend was largely driven by changes in the subtropical gyres. Both Polovina et al. (2008) and Irwin and Oliver (2009) noted ENSO or PDO-associated increases in the areal extent of the most oligotrophic water in subtropical gyres. Finally, recent analyses of ocean color data from 1997 to 2010 and 1997 to 2013 suggest gradual, yet significant, decreases in surface chl *a* in subjectively defined polygons that encompassed the oligotrophic regions of the North Pacific as well as other basins (Signorini and McClain, 2012; Signorini et al., 2015). Conversely, Siegel et al. (2013) argue that the tropical/sub-tropical negative correlation between satellite chl *a* and sea surface temperature (SST) is primarily a physiological signal of variable chl *a* to carbon (C) ratio rather than a phytoplankton biomass signal, likely associated with photoacclimation (Letelier et al., 1993, 2017; Winn et al., 1993). While some analyses of long-term *in situ* data support the trend toward oligotrophy found in early large-scale studies (Boyce et al., 2010, 2011, 2014), the majority of *in situ* time series do not (Chavez et al., 2011; McQuatters-Gollop et al., 2011).

Contrary findings between gyre-scale and *in situ* analyses, attribution of change to differing climate modes, and the variations in the shape and extent of the gyre suggest that regional oceanographic context needs to be considered when examining the role of interannual variability and secular trends on large scale shifts in the subtropical gyres (e.g., Hammond et al., 2017). One such regional approach considers the temporal patterns of features as a composite of biophysical interactions (Oliver and Irwin, 2008; Kavanaugh et al., 2014b, 2016). Seasonally evolving satellite-derived seascapes describe regional variability in the North Pacific with differences in biogeochemical interactions (Kavanaugh et al., 2014b), and community structure (Kavanaugh et al., 2014a). Here, we use interannual varying seascapes to further our understanding of subtropical gyre dynamics and compare seascape variability relative to circulation-based or low-level chl *a*-based definitions of the gyre. We hypothesized that year-to-year variability in the size of the subtropical gyre and location of the gyre boundary is reflected in the patterns of phytoplankton abundance and productivity at Station ALOHA. The location of Station ALOHA is highlighted, with trends and oscillations of seascape area and isolation compared across definitions and analyzed in concert with *in situ* patterns. Specifically, we address the following questions:

1. What are the interannual trends across different metrics of gyre expansion?
2. To what degree are variations in subtropical seascape geography related to interannual to decadal climate modes?
3. Finally, how do variations in seascape geography relate to the interannual patterns of phytoplankton abundance and primary productivity observed at Station ALOHA?

METHODS

Oligotrophic Chl *a* Gyre Extent

Area of the extent of highly oligotrophic gyre (a threshold defined as chl $a \leq 0.07$ mg m^{-3}; Polovina et al., 2008, hereafter oligotrophic threshold chl *a*) was calculated from monthly

SeaWiFS (R2017, completed January 2018) and Aqua-MODIS (R2017, completed December 2017) satellite ocean color derived chl *a* (**Figure 1A**). The SeaWiFS data record extends from autumn of 1997–2010 albeit with episodic gaps during 2008–2010 due to periodic sensor malfunction. Reprocessing (Franz et al., 2007; Franz, 2009) has removed much of the drift in the SeaWiFS and Aqua-MODIS instruments. Data were merged by comparing the per pixel seasonal cycle of SeaWiFS to that of MODIS-Aqua from 2003 to 2007, and then applying a seasonal correction to the historical SeaWiFS record. Merged data include seasonally adjusted SeaWiFS data until July of 2002, after which MODIS-Aqua data were used to December 2016. We also compared the trends between the OCI algorithm (Hu et al., 2012) to that of the previously standard OC3/OC4 (OCX) algorithms for SeaWiFS and MODIS-Aqua. The OCI algorithm is more accurate for [chl *a*] <0.2 mg m^{-3}, converges with the OCX values above 0.2 mg m^{-3}, and has been the standard NASA chl *a* algorithm since 2014.

Circulation-Based Gyre Extent and Eddy Kinetic Energy

Near daily, gridded sea level anomalies (SLA) and absolute dynamic topography (ADT) fields derived from satellite altimetry were downloaded from AVISO (https://www.aviso.altimetry.fr/en/data/products.html). Eddy kinetic energy (EKE) was calculated from the near daily fields:

$$\mathrm{EKE}\ (\mathrm{m}^2\ \mathrm{s}^{-2}) = 0.5 \times [u^2 + v^2] \quad (1)$$

where u and v are the zonal and meridional velocities calculated from sea surface height anomalies. Monthly means of each field were calculated.

Because the determination of extent of features estimated from geostrophic flow lines can be confounded by the effect of steric sea level rise on ADT (Gille, 2014), we downloaded steric sea level anomalies (Levitus et al., 2012) for the upper 2,000 m from NOAA's National Center for Environmental Information (https://www.nodc.noaa.gov/OC5/3M_HEAT_CONTENT/index.html), and calculated the trend in steric sea-level rise from 1993 to 2015 on a per pixel basis. Dynamic height was adjusted by subtracting the interpolated steric sea-level trend from the monthly satellite dynamic height field. The gyre was then classified as the region contained within closing contours of original ADT and adjusted ADT (ADT_adj) at 1.05 m, the minimum height at which the contour lines recirculated (closed) completely to the western boundary (**Figure 1B**).

Seascape Classification

Seascapes were classified from Level 3 9-km merged chl *a* (described above), PAR, and SST from the Advanced Very High Resolution Radiometer (AVHRR) and MODIS-Aqua. Similar to chl *a*, monthly averages of PAR and SST were computed from the combined SeaWiFS and MODIS product; all three variables were binned to 1 degree to match model output. Model output of SST, PAR, and surface chl *a* from 1985 to 2005 were taken from the Biogeochemical Element Cycling Model embedded

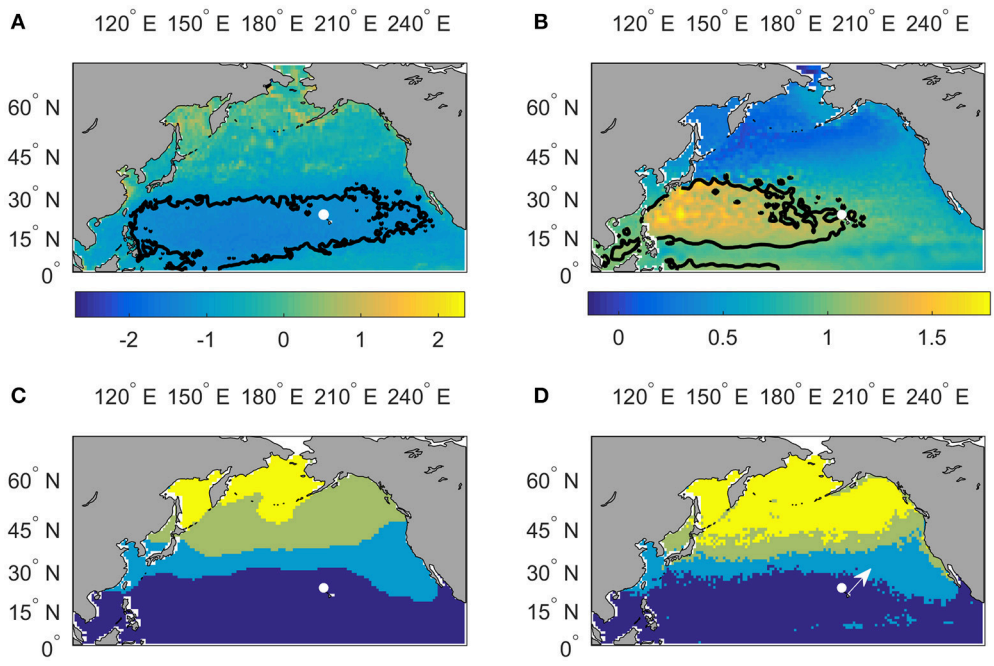

FIGURE 1 | Extent of the North Pacific Subtropical Gyre (NPSG) for June of 2003, showing **(A)** oligotrophic threshold ($\leq$0.07 mg m^{-3}) satellite ocean color derived surface chlorophyll, chl *a*; **(B)** geostrophic recirculation defined by the 1.05 m absolute dynamic height relative to the geoid; and multivariate seascapes classified from **(C)** CESM-BEC model output and **(D)** satellite data. Dark blue, subtropical seascape; light blue, oligotrophic boundary seascape; green, transition seascape; yellow, subarctic seascape. Arrow in **(D)** shows distance between Station ALOHA (white circle) and the boundary of the subtropical seascape.

in the Community Earth System Model (CESM-BEC, Doney et al., 2009; Moore et al., 2013). Surface chl *a* concentration is sensitive to mixed layer depth in the subtropics (e.g., Letelier et al., 1996; Siegel et al., 2013); thus we chose the CESM-BEC because of its inclusion of photoacclimation. While this does not isolate the effect of photoacclimation, it assures that modeled chl *a* and satellite chl *a* are responding similarly to physical forcing, reflecting the phytoplankton physiological responses observed at Station ALOHA. All data sets were standardized prior to classification. Satellite and model seascapes were classified separately (**Figures 1C,D**).

Climatological seasonal means of PAR, SST, and chl *a* were defined for both data sets from 2003 to 2007. We used a probabilistic self-organizing mapping algorithm (PrSOM, Anouar et al., 1998) to reduce the 3-variable (SSTx,y,m, PARx,y, chl *a* x,y,m) spatiotemporal data set onto a 15 × 15 neuronal map resulting in 225 classes, each with its own 3-D weight based on the maximum likelihood estimation (3-D MLEs). The neural net size (15 × 15 nodes) was chosen to maximize sensitivity to mesoscale processes while preventing underpopulated nodes (defined as <500 pixels). The 3-D MLEs were then further reduced using a hierarchical agglomerative clustering (HAC) with Ward linkages (Ward, 1963). This linkage method uses combinatorial, Euclidian distances that conserve the original data space with sequential linkages (McCune et al., 2002). Euclidian distances here are equivalent to within-group and total sum of squares.

Previously, we found that eight seascapes classified from seasonal climatologies of satellite-derived SST, chl *a*, and PAR represented seasonal shifts in biogeochemical patterns and planktonic assemblages (Kavanaugh et al., 2014a,b). Here, we followed the methodology of Kavanaugh et al. (2014b), with three exceptions. First, the seasonal variability of PAR was removed on a per-pixel basis to minimize discontinuities associated with the spring and fall transitions, with interannual and spatial variability remaining. Second, stepwise agglomerations were conducted using the Ward method until four seascapes for each of the model and satellite data sets were defined: a subtropical seascape, oligotrophic transition, a mesotrophic transition, and a subarctic seascape. These four regions bear the spatial signature of analogous seasonally evolving regions classified previously (Kavanaugh et al., 2014b) and represent a trade-off between variance explained in both the satellite and model records, and spatial match-up between satellite and modeled seascapes (**Figure S1**). Finally, once the seasonal and spatial vectors were classified, the means, variances and covariances within seascapes informed a multivariate Gaussian mixture model (GMM). Class assignments of individual months were then determined by their maximum posterior probabilities. New classes were then predicted from the CESM and satellite GMMs using the monthly means of chl *a*, SST, and PAR of the respective model and satellite time series.

Geographic Metrics

We focus on the dynamics of the subtropical seascape and the boundary between the subtropical and oligotrophic transition seascape. Total area of oligotrophy, recirculation, and multivariate subtropical seascape was assigned based on the sum of the area of all pixels within the appropriate contour or identified seascape in the North Pacific. Surface area of each pixel was calculated by correcting for the spheroid-effect on distance between lines of longitude. For each time step, the distance from Station ALOHA to the subtropical seascape boundary was also calculated using the mean of the 5th quantile of all boundary distances in a quadrant 45° on either side of due NE from Station ALOHA **Figure 1D**); encroachment of less oligotrophic waters from the NE was most common. When the oligotrophic boundary encroached beyond (south and or east of) Station ALOHA, the distance values were negative. All area-based analyses were truncated at 10°N to minimize the effect of the equatorial upwelling region.

To understand the role of mesoscale variability on basin-scale geography, we examined the relationship between mean EKE and the difference in extent between the gyre defined by circulation and that defined by oligotrophy (see above). Pixels were categorized as belonging in (1) both the oligotrophic and physical gyres, (2) only in the physical gyre, or (3) only in the oligotrophic gyre. The mean EKE was calculated over the pixels for each of the three aforementioned groups.

Climatic Indices

To infer the effect of climatic forcing on the interannual dynamics of gyre geography, three different indices were used. The multivariate El Niño Southern Oscillation Index (MEI) is computed from a principal component analysis (PCA) of six variables including sea level pressure, zonal and meridional wind components, cloudiness, and sea surface and air temperatures (Wolter and Timlin, 1993). These data are available from NOAA (http://www.esrl.noaa.gov/psd/enso/mei/). The North Pacific Gyre Oscillation (NPGO, Di Lorenzo et al., 2008; http://www.o3d.org/npgo/) is the second dominant mode calculated from North Pacific sea surface height anomalies and is associated with accelerated North Pacific, Alaska, and California Currents (Chavez et al., 2011). The Pacific Decadal Oscillation (PDO, Mantua et al., 1997; Zhang et al., 1997) is associated with the dominant mode of North Pacific SST anomalies and the data are available from the University of Washington (http://jisao.washington.edu/pdo/).

Station ALOHA Data

In situ NPP, Total chl *a* (Tchl *a*, the sum of divinyl and monovinyl chl *a*), and *in situ* physical patterns in the subtropical North Pacific were assessed using archived data from Station ALOHA (http://hahana.soest.hawaii.edu/hot/hot-dogs/interface.html). Net PP was determined by daytime incubation in bottles spiked with ^{14}C bicarbonate incubated *in situ* to maintain natural light and temperature (Letelier et al., 1996). Chl *a* and photosynthetic accessory pigments were measured by high performance liquid chromatography (HPLC) according to Wright et al. (1991). Mean pigment concentrations and NPP patterns were quantified separately for the light-saturated surface (0–45 m) and light-limited region of the euphotic zone that contained the deep chlorophyll maximum (DCM, 75–150 m). Potential temperature and bottle salinity were also recorded for the upper 45 m. Mixed layer depth was calculated using

a potential density gradient threshold of 0.005 kg m^{-4} and a potential density offset of 0.125 kg m^{-3} from the surface (Karl and Lukas, 1996).

Statistical Analysis

Cross correlation analyses were conducted to determine the correlations between climate and geographic metrics, the relationship between seascape dynamics and *in situ* conditions at Station ALOHA, and the time scales or lags at which the correlation was strongest. Cross correlation analysis was also conducted to determine the effect of EKE on spatial mismatch between geographic metrics. Prior to analysis, monthly climatological means were calculated by removing outliers (exceeding $\pm$ 3 standard deviations), then missing *in situ* data were interpolated using a 3-month LOESS filter to minimize the effect of within-year data density on interannual trends. Then, anomalies for each time series were calculated by subtracting the monthly climatological mean, calculated from the smoothed data, and then smoothing with a 12-month LOESS filter prior to correlation analysis. Statistical significance of correlation coefficients were determined using a critical value which adjusted degrees of freedom to account for autocorrelation in covariance (Glover et al., 2011). Correlations that exceeded this value are considered significant ($p < 0.05$).

Trends over time were adjusted to account for the effect of climate oscillations. We conducted a PCA across the NPGO, PDO, and MEI indices; multiple linear regression was conducted using the PCA scores as predictors and individual seasonally-detrended anomalies as responses. Trends were then a result of a simple linear fit to the residuals of the multiple linear regression model.

RESULTS

Climate Variability

From 1985 to 2016, three to four cycles of the NPGO, MEI, and PDO were evident (**Figure 2**). In the early part of the record (1985–1998), the PDO and MEI were out of phase but moved into phase following the 1997–1998 El Niño and subsequent La Niña, remaining in phase for the rest of the data record ($r = 0.6$, $p < 0.001$). Throughout our study period, the NPGO was anticorrelated ($r = -0.5$, $p < 0.001$) with the other two indices, but also led the PDO and MEI by 5 and 8 months, respectively (**Figure S2**). Thus, any secular trend reported is that which remains after accounting for the effect of oscillations in the sign and magnitude of the climate indicators.

Expansion and Isolation Trends and Drivers

Patterns and trends among the different gyre geographic metrics varied and were associated with different climate forcing. The area of low-level chl *a* was dependent on algorithm, with the lower sensitivity of the OCX resulting in a larger expanse of oligotrophy (**Figure 3A**, **Table 1**). Large interannual oscillations were evident, with any linear trend being highly dependent on record length (**Table S1**). From 1998 to 2016, expansion of the area of low-level chl *a* occurred at a rate of 0.36% $year^{-1}$ (**Table 1**). Seasonal and interannual oscillations as well as weak increases (0.5% per year) in the physical extent of the gyre were evident from the altimetry-based time series (**Figure 3B**, **Table 1**). Trends were weaker in data adjusted for steric sea-level changes than those unadjusted for absolute dynamic height (ADT_adj and ADT, respectively, **Table S1**). As with the extent of oligotrophy, presence or magnitude of a trend depended on the length of the time series, with no trend evident from 1998 to 2006 (**Figure 3B**, **Table S1**), despite the strong ENSO signal during that span. Because modeled and satellite seascapes were highly correlated and in phase for both indices (**Figures S1B,C**; expansion: $r = 0.64$, $p < 0.05$; isolation $r = 0.76$, $p < 0.05$), the data records were combined and a single index of expansion or isolation was used that spanned the entire data record (1985–2016). There was evidence of slight expansion of the subtropical seascape from 1985 to 2016 (**Table 1**). Isolation distance also varied from year to year, although aseasonal, within-year variability was higher relative to the other metrics (**Figure 3D**). A linear trend was evident from 1985 to 2016 (but not over a shorter duration), with isolation distance increasing by 0.9% per year (**Table 1**).

Gyre extent, defined by oligotrophic threshold chl *a*, was positively correlated to the MEI, with positive MEI preceding expansion of low-level chl *a* area by 6–12 months (**Figure 4A**). The areal extent of recirculation was positively correlated with the NPGO and strongly negatively correlated with the PDO and MEI (**Figure 4B**). Similar to the area of low-level chl *a*, the subtropical seascape was strongly correlated to the MEI and was also related to the PDO (**Figure 4C**), whereas the isolation of Station ALOHA within the subtropical gyre was positively correlated with the NPGO and negatively correlated with the MEI and PDO (**Figure 4D**). While covering a much larger area, areal extent of multivariate seascapes was weakly correlated to that of threshold chl *a* patterns, (**Figure S3A**: $r = 0.24$, $p < 0.05$); however, patterns preceded the chl-only index by approximately 7 months. Multivariate seascape expansion was anti-correlated to both the dynamic topography extent described above ($r = -0.48$, $p < 0.05$), and the distance of Station ALOHA to the edge of the subtropical seascape (**Figure S3B**: $r = -0.36$, $p < 0.05$). Isolation distance was positively correlated to gyre extent as measured by geostrophy ($r = 0.33$, $p < 0.05$), with isolation shifts preceding that of gyre extent also by 7 months. Isolation was not correlated to the low-level chl *a* metric.

The NPSG is most contracted in winter and at its greatest extent in September for both definitions of the gyre (**Figures 5A,B**). The northern winter boundary of the physical gyre exceeds that of low-level chl *a*, and the summer eastern boundary extends less than the low-level chl-a. However, on interannual scales, the physical extent and low-level chl *a*-based extent were anti-correlated, due to different climate forcing. The physical extent is strongly positively correlated with the NPGO, whereas the extent of low-level chl *a* is positively correlated with the PDO and MEI. Increased EKE resulted in expansion of the areal extent of oligotrophic-threshold chl *a*. The result is that off of the Kuroshio, the spatial mismatch between the two definitions is minimized with increased EKE between their boundaries (**Figure 5C**),

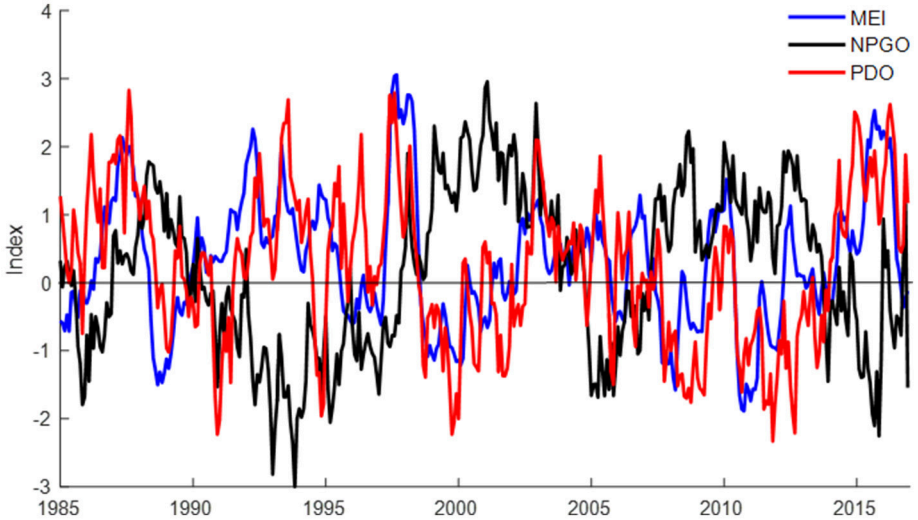

FIGURE 2 | Time series of climate indices including (a) the North Pacific Gyre Oscillation, NPGO; (b) the Multivariate ENSO Index, MEI; and (c) the Pacific Decadal Oscillation, PDO. Data sources are included in Methods. All series were smoothed using a 12-month LOESS filter.

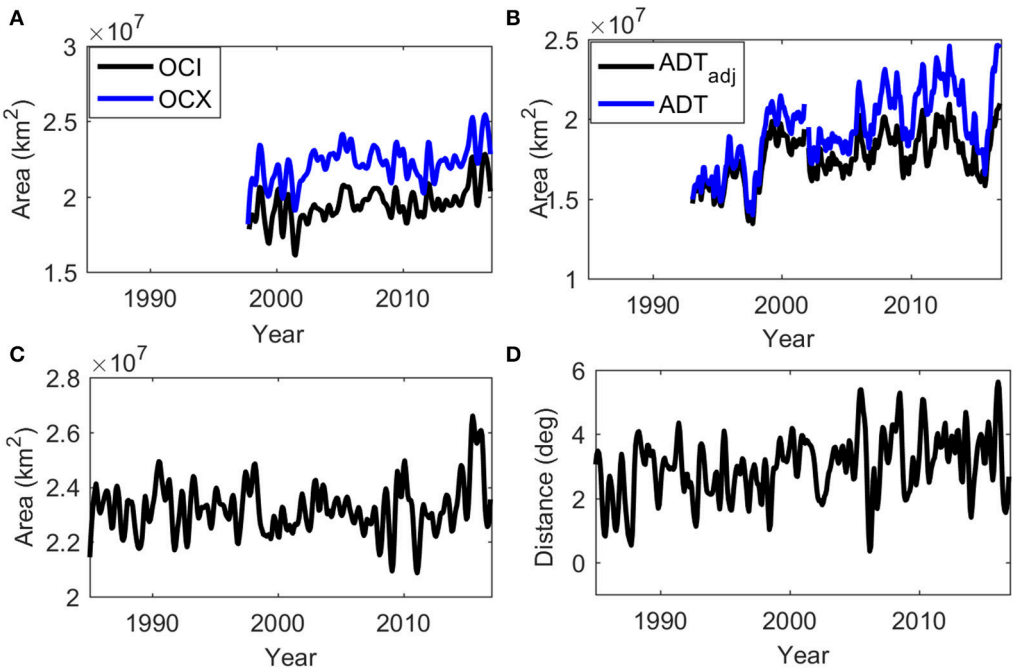

FIGURE 3 | Temporal trends of North Pacific subtropical gyre dynamic geography indices showing **(A)** areal extent calculated from oligotrophic threshold chl *a* across different satellite ocean color algorithms; **(B)** areal extent (expansion/contraction) calculated from satellite altimetry derived dynamic topography with and without adjustment for steric sea-level rise; **(C)** merged model and satellite seascape extent; **(D)** distance of Station ALOHA to the edge of the merged modeled and satellite subtropical seascape (isolation). All series were smoothed using a 12-month LOESS filter. Trends calculated over various durations are reported in **Table 1** and **Table S1**.

where instabilities associated with the Kuroshio extension appeared to blend the physical and chl *a*-based boundaries. On the eastern and southern edge, the spatial mismatch increases with increased EKE (**Figure 5D**), where expanded oligotrophy is associated with greater EKE, particularly in summer.

In Situ Trends

Local SST averaged over the upper 45 m at Station ALOHA exhibited strong oscillations in response to changing climate forcing over the data record, with warmer temperatures associated with positive ENSO and PDO and negative NPGO (**Figure 6A**, **Figure S4**). While there was a significant linear

TABLE 1 | Secular trends across geographic metrics, chl *a* algorithms, and *in situ* characteristics at Station ALOHA.

Algorithm	Span	Span mean	Trend (year^{-1})	Trend (SE)	% change year^{-1}	R^2	*p*-Value
AREA METRICS (km^2)							
ocx: chl *a* ≤0.07 mg m^{-3}	1998–2016	2.23E+007	*4.87E+04*	1.39E+04	0.220	0.05	<0.001
oci: chl *a* ≤ 0.07 mg m^{-3}	1998–2016	1.95E+007	7.00E+04	1.36E+04	0.360	0.11	<0.001
ADT_adj	1993–2016	1.76E+007	8.66E+04	1.11E+04	0.491	0.42	<0.001
ADT_adj	1998–2016	1.76E+007	8.48E+04	1.08E+04	0.481	0.27	<0.001
Subtropical Seascape	1985–2016	2.32E+007	1.64+04	6.03E+03	0.071	0.02	<0.01
DISTANCE METRICS (km)							
Station ALOHA to SS edge	1985–2016	3.28E+02	3.20E+00	8.90E-01	0.970	0.04	<0.001
STATION ALOHA							
SST (°C)	1989–2016	24.8	0.013	0.004	0.052	0.04	<0.01
SSS (psu)	1989–2016	35.1	0.008	0.001	0.023	0.14	<0.001
MLD (surface offset, m)	1989–2016	58.7	0.29	0.13	0.494	0.02	0.02
MLD (gradient threshold, m)	*1989–2016*	*32.5*	*0.14*	*0.11*	*0.431*	*0*	*0.2*
[chl *a*]: 0–45 m (mg chl *a* m^{-3})	*1989–2016*	*0.09*	*0*	*0*	*0.000*	*0*	*0.72*
[chl *a*]: 75–150 m (mg chl *a* m $^{-3}$)	1989–2016	0.17	0.001	0.0002	0.588	0.06	<0.001
NPP: 0–45 m (mg C m^{-3} d^{-1})	1989–2016	6.07	0.053	0.01	0.873	0.08	<0.001
NPP: 75–150 m (mg C m^{-3} d^{-1})	1989–2016	1.13	0.045	0.004	3.982	0.34	<0.001
NPP: Int to150 m (mg C m^{-2} d^{-1})	1989–2016	513	5.63	0.85	1.097	0.18	<0.001

Italicized values denote no significant trend over the duration measured. Signatures of the NPGO, PDO, and MEI have been removed from each time series prior to analysis (see section Methods).

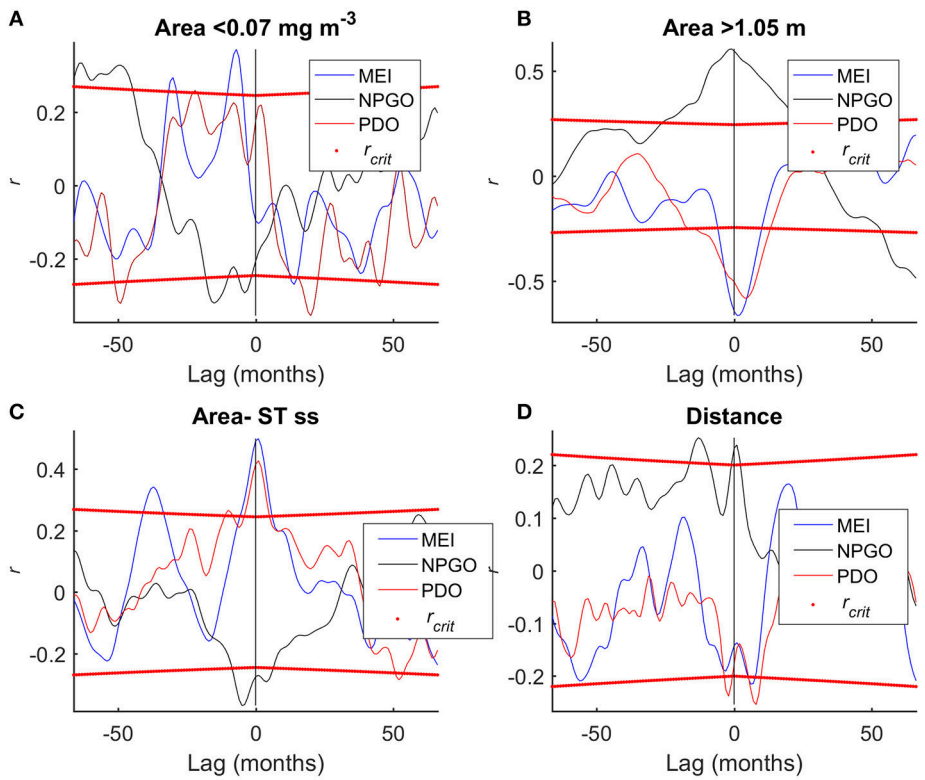

FIGURE 4 | Lagged correlations between climate indices and dynamic geography indices of the North Pacific Subtropical Gyre. Where lag is negative, climate index leads geographic metric; the converse is true for positive lags. Correlations are significant when they exceed the critical value (dotted red lines). **(A)** Gyre area defined by chl *a* ≤ 0.07 mg m^{-3}. **(B)** Gyre area defined by closing contour of dynamic height (1.05 m). **(C)** Gyre area defined by the extent of the multivariate subtropical seascape. **(D)** Distance from Station ALOHA to the edge of the subtropical seascape.

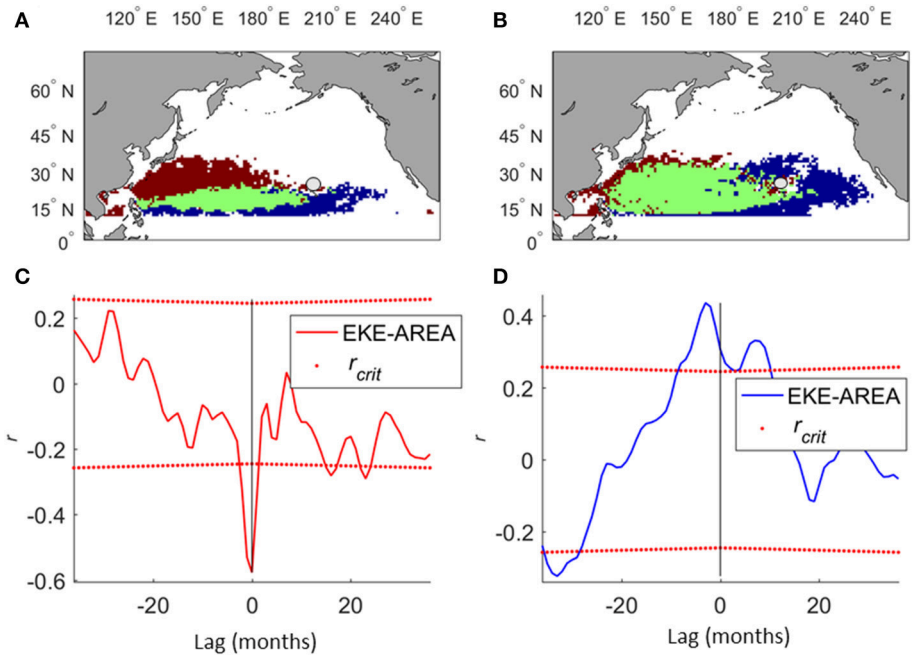

FIGURE 5 | Drivers of spatiotemporal differences in gyre extent based on dynamic height and oligotrophic threshold chl *a*. **(A)** Extent of gyre in February 2003 showing topographic (red) and pigment (blue)- based extents and region of overlap (green). **(B)** Same as **(A)**, but for September 2003. **(C)** Cross correlation of mean eddy kinetic energy (EKE) in region represented solely by the physical definition with areal extent of that region. **(D)** Same as **(C)**, but in extents solely represented by oligotrophic threshold chl *a*.

trend from 1989 to 2016 (**Table 1**: 0.010 ± 0.004°C year^{-1}, $p < 0.01$), it was very weak ($R^2 = 0.04$). Sea surface salinity exhibited large oscillations in the opposite direction of SST and also a relatively strong increasing trend over the data record (0.008 ± 0.001 psu year^{-1}, $p < 0.001$, $R^2 = 0.18$; **Figure 6B**). Mixed layer depth had large interannual variability over the data record, but also oscillated in response to changing surface salinity and temperature. A weak linear increase was apparent over the data record for mixed layer calculated via the surface offset method (0.29 ± 0.13 m year^{-1}, $p = 0.02$, $R^2 = 0.02$; **Figure 6D**), although none was apparent with the mixed layer depth calculated via the gradient method (**Figure 6C**, **Table 1**).

With the exception of isolated events (e.g., early 2001), seasonal patterns of T-chl *a* in the surface and at depth were out of phase (**Figure 7A**). Concentrations in the light-limited euphotic zone were approximately double that of the surface, and also increased over the data record (**Table 1**: 0.001 ± 0.0002 mg chl *a* m^{-3} year^{-1}, $p < 0.001$, $R^2 = 0.08$). No analogous trend was evident in surface chlorophyll.

NPP increased over the data record in both the surface and at depth (**Figure 7B**, **Table 1**). Mean rates in the surface were ∼4x higher than that in the 75–150 m depth bin (**Table 1**: 5–7 mg C m^{-3} d^{-1} vs. 1–2 mg C m^{-3} d^{-1}). However, the relative rate of increase in NPP over time was stronger in the light limited euphotic zone vs. the surface (**Table 1**: surface ∼1% year^{-1}, trend = 0.053 ± 0.010 mg C m^{-3} d^{-1}year^{-1}, $p < 0.001$, $R^2 = 0.09$; At depth ∼3% year^{-1}, trend = 0.045 ± 0.004 mg C m^{-3} d^{-1}year^{-1}, $p < 0.001$, $R^2 = 0.34$). Together, these trends contributed to a relatively strong linear increase in NPP integrated over 150 m (**Figure 7C**, 5.63 ± 0.85 mg C m^{-2} d^{-1}year^{-1}, $p < 0.001$, $R^2 = 0.18$). Oscillations were also evident in both chl *a* and NPP time series.

Correlation of Seascape Geography With *in Situ* Physics and Biology

Increased mixed layer depth followed isolation of Station ALOHA (**Figure 8A**, $r = 0.32$, $p < 0.05$) and preceded a contracted subtropical seascape (**Figure 8B**, $r = -0.32$, $p < 0.05$) by ∼6 months. Salinity was positively associated with isolation but at longer lags ($r = 0.28$–0.32, lags > 20 months) and negatively associated with, but preceding expansion of the subtropical seascape ($r = -0.35$, $p < 0.05$, ∼1year). SST was positively associated with subtropical seascape expansion (**Figure 8B**), but preceded expansion by ∼1 year ($r = 0.3$, $p < 0.05$). These patterns generally followed what would be expected by the climate forcing of geography (**Figure 4**, **Figure S4**) with SST at Station ALOHA positively correlated with the PDO and MEI (and negatively with the NPGO), and surface salinity and mixed layer depth positively correlated with the NPGO (and negatively correlated with the PDO and MEI) (**Figure S4**). Time lags and wavelengths were much longer and broader when considering climate indices directly, rather than their geographic signatures.

Station ALOHA T chl *a* and NPP were also correlated to gyre geography following local physical forcing. Isolation was

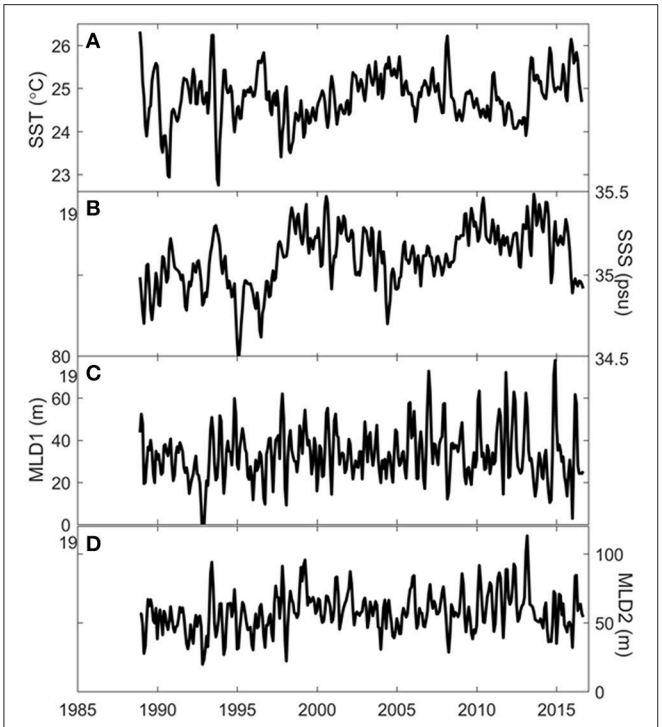

FIGURE 6 | *In situ* surface conditions at Station ALOHA showing anomalies for **(A)** sea surface temperature (SST); **(B)** sea surface salinity; **(C)** mixed layer depth as defined by a vertical gradient threshold of 0.005 kg m^{-3} m^{-1} for potential density and **(D)** mixed layer depth as defined by a density surface offset of 0.125 kg m^{-3}.

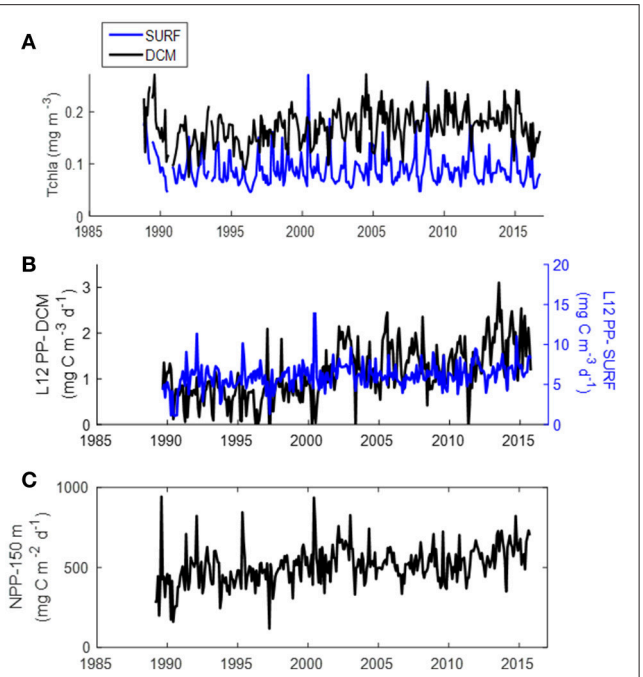

FIGURE 7 | Phytoplankton dynamics at Station ALOHA showing anomalies for **(A)** T chl *a* in the surface and deep chlorophyll maximum, DCM, **(B)** Net primary productivity in the surface (0–45 m) and depth (75–150 m) as calculated from daytime incubations, and **(C)** vertically integrated NPP from 0 to 150 m.

associated with increased chl *a* in the surface (**Figure 8C**, $r = 0.32$, $p < 0.05$), and increased surface and integrated NPP (**Figure 8E**, $r = 0.32$ to 0.4, $p < 0.05$) followed isolation by ∼5 months. Decreased Tchl *a* at depth was strongly associated with expansion of the subtropical seascape (**Figure 8D**: $r = -0.41$, $p < 0.05$) as was decreased NPP throughout the water column (**Figure 8F**: $r = -0.28$ to -0.39, $p < 0.05$).

DISCUSSION

Where satellite metrics have suggested that oligotrophic systems such as the NPSG will expand in response to warming oceans (Behrenfeld et al., 2006; Polovina et al., 2008; Irwin and Oliver, 2009), analogous changes have not been evident at Station ALOHA (Corno et al., 2007) or the Bermuda Atlantic Time-series Station BATS in the subtropical North Atlantic (Lomas et al., 2010). This suggests that there may be physiological or structural reorganization not observed from space, uncharacterized spatiotemporal variability, or satellite sensor drift. We examined the geographic dynamics of the NPSG, the role of climate forcing on those dynamics, and the relationships between shifting gyre geography and local *in situ* conditions at the long-term time-series station, Station ALOHA over a 31-year data record. While weak secular trends in the expansion of different metrics of the subtropical gyre were evident, they were dominated by large oscillations, correlated with changes in ENSO and PDO conditions as well as the NPGO. With oscillations, we observe that *in situ* biophysical conditions at Station ALOHA are congruent to what would be predicted during periods of expanded oligotrophy via an expanded subtropical seascape including warmer SST and declines in T chl *a* and NPP. We also observe that conditions at Station ALOHA shift prior to multivariate seascape expansion, suggesting that Station ALOHA may serve as a leading indicator for changes throughout the North Pacific subtropical region.

The location of Station ALOHA at the edge of the subtropics (this study) and other pivot points of climate forcing (Chavez et al., 2011; Messié and Chavez, 2011) may result in different climate effects depending on the interaction of multiple climate modes. During positive ENSO phases, water column stabilization restricts upward mixing of new nitrate and selects for organisms that can fix atmospheric nitrogen (Karl et al., 1995, 2001; Campbell et al., 1997). During positive PDO, the Aleutian Low is further south and leads to a southern anomaly in the transition zone chlorophyll front and potentially higher than average primary productivity in the subtropics (Chai et al., 2003). Positive NPGO periods are associated with more northward Aleutian Lows (Chavez et al., 2011) along with stronger North Pacific and California currents, higher pressure and deeper thermocline depths at the center of the subtropics (Di Lorenzo et al., 2008, 2009), potentially leading to decreased access to

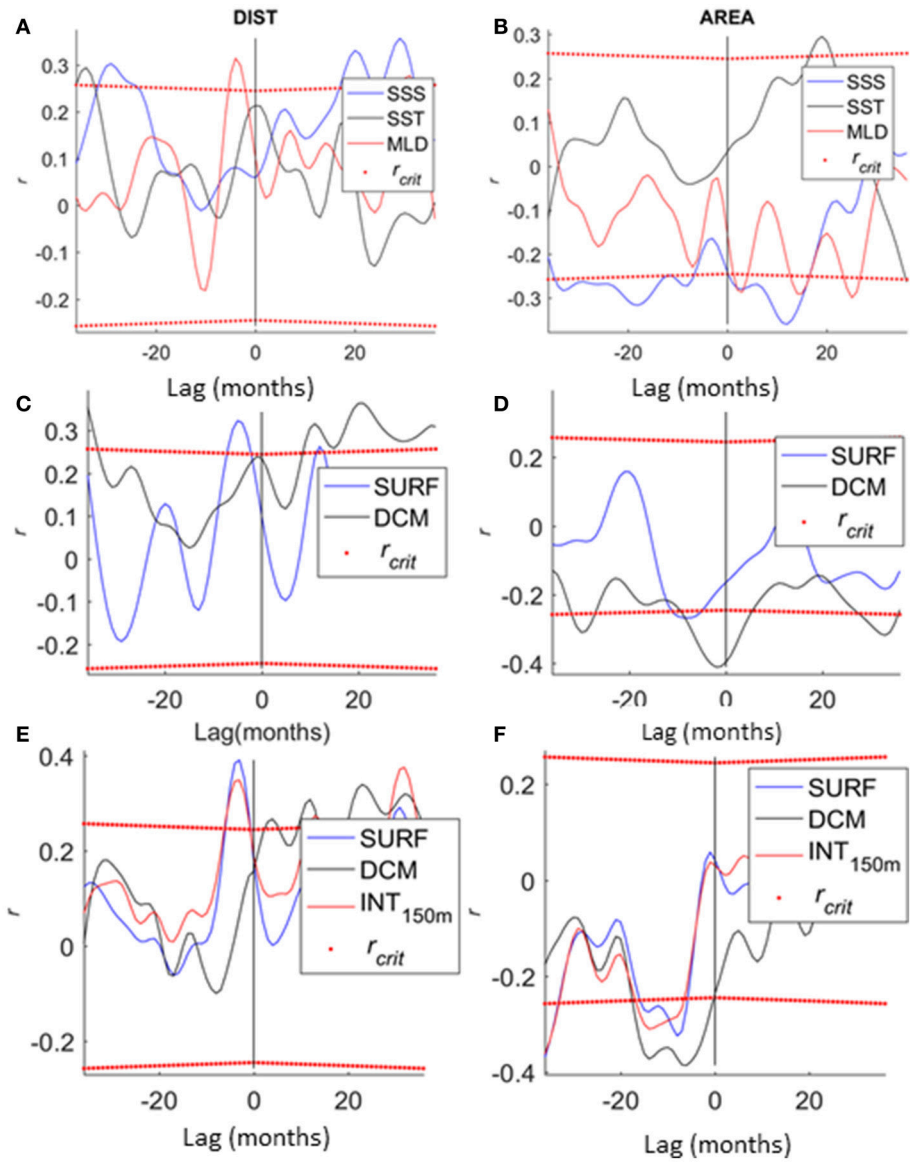

FIGURE 8 | Correlation between *in situ* biophysical variables at Station ALOHA and isolation of Station ALOHA (DIST) and expansion of subtropical seascape (AREA). **(A,B)** SST, mixed layer depth, and salinity; **(C,D)** Tchl *a* in the surface and DCM; **(E,F)** NPP in surface, DCM, and integrated over the upper 150 m. Geographic metrics lead biophysical variables when lag is negative.

deep nutrients in the interior of the gyre. However we found that positive phases of the NPGO were associated with increased mixed layer depth, salinity, and isolation of Station ALOHA which preceded increased T chl *a* and NPP. Conversely, the subtropical seascape (as well as the extent of oligotrophy defined solely by the threshold chl *a*) were associated with positive phases of the MEI and PDO, a shoaling and freshening mixed layer, and declines in T chl *a* and NPP at Station ALOHA. Thus while a stronger gyre may result in decreased access to nutrients at the center of the gyre (Di Lorenzo et al., 2008), the positive NPGO may result in increased access to nutrients at the edge. Furthermore, changes of biological and physical properties at Station ALOHA tend to precede expansion by a few months. Thus, despite its location on the northeastern edge of the NPSG, or perhaps because of it, the time-series station provides an early indication of biogeographic conditions of the gyre as a whole.

The expansion of the topography-defined gyre positively correlated with the NPGO, and negatively correlated with MEI, PDO, and the gyre defined by the 0.07 mg chl *a* m^{-3} threshold. Isolation of Station ALOHA (the distance to the NE boundary of the most oligotrophic seascape) also was related to the NPGO (was positively correlated but led geostrophic expansion by 7 months) and exhibited a weak trend toward increased isolation

over the duration of the study. During positive NPGO conditions, transport through the North Pacific and California currents is stronger (Di Lorenzo et al., 2008), and meanders of the southern edge of the North Pacific Current-California current bifurcation may be reduced leading to the associated increase in isolation of Station ALOHA within the northeast corner of the subtropical seascape.

Eddy kinetic energy appears to expand the geographic signature of oligotrophy, resulting in a temporal mismatch between the gyre defined by low-level chl *a* and dynamic topography. While this suggests that the net effect of mesoscale processes on chl *a* (extent of oligotrophy) is negative (expansive), the observed effect of eddies on phytoplankton biomass and NPP near Station ALOHA are mixed. Upwelling within cyclonic eddies have also been purported to change community structure (Bidigare et al., 2003), primary and new production (Vaillancourt et al., 2003). Anticyclonic eddies can result in increased nitrogen fixation (Fong et al., 2008; Church et al., 2009) which is responsible for over 40% of the new/export production at HOT. Finally, regions between anticyclonic and cyclonic eddies have also been shown to have increased PP and particulate organic carbon flux (Guidi et al., 2012). Sea surface height variation in general, has been found to affect the location and species composition in the DCM, with a shallower DCM with higher abundance of larger eukaryotic phytoplankton occurring with lower SSH (Barone et al., in review). Future studies could use existing databases to investigate the relative frequency of eddies (e.g., Chelton et al., 2011) in the NPSG during different climate modes, and determine whether changes in frequency are accompanied by changes in nitrogen fixation, NPP, and export at Station ALOHA.

Secular increases in the gyre geographical extent are weak, but evident within all four geographic indices. Limited by the satellite record at the time of publication, Polovina et al. (2008) reported increases in the areal extent of oligotrophic threshold chl *a* in the North Pacific at a rate of 2.2% per year from 1998 to 2007. Irwin and Oliver (2009) reported general increases through time in the most oligotrophic provinces in their classification, with oscillatory behavior found across all oligotrophic provinces. Using a longer record and linear regression analyses, Signorini et al. (2015) found mostly secular declines in surface chl *a* over large, subjectively chosen regions, but also discussed the influence of mixed layer depth changes and subsequent photoacclimation on chl *a* in the subtropics. In our re-analysis of geographic trends in the North Pacific using the latest processing of MODIS and SeaWiFS, we observe ENSO- and PDO-influenced oscillations of areal extent of regions with chl *a* $<0.07\,mg\,m^{-3}$ over a weak secular trend (**Figure 3A**, **Table 1**); however, we derive much slower rates of expansion than previously reported. Reprocessing and subsequent lowering of blue water chl *a* concentrations in the early SeaWiFS record (https://oceancolor.gsfc.nasa.gov/reprocessing/r2014/seawifs/) may be one reason for this discrepancy in expansion rate (2–1.1%). However, the chl *a* algorithm used (a decline of 1.1–0.7% $year^{-1}$) and a data record length that could account for climate oscillations (a decline from 0.7 to 0.4% $year^{-1}$) may contribute to a greater extent. Nevertheless, the gyre as defined by dynamic topography also appears to be expanding, and relatedly, increasing the isolation of Station ALOHA. Physical gyre expansion was fastest prior to 1998, but appeared to increase throughout the altimetry record even with adjustments made for steric sea level rise (e.g., Gille, 2014). Note that surface topography in our analysis has not been corrected for interannual variability in atmospheric pressure; for this reason our reported trends based on SSH must be viewed as preliminary. Finally, we see no secular trend, but strong oscillations and correlation with both ENSO and PDO were apparent with the extent of the multivariate subtropical seascape (**Figures 3C**, **4C**), where chl *a* dynamics may have been balanced in the classification by SST and spatial light variability. The latter result is in agreement with Behrenfeld et al. (2016), who found large oscillations in surface chl *a* concentrations in the subtropical gyres after accounting for the effect of photoacclimation.

After accounting for climate oscillations in the *in situ* data record at Station ALOHA, we observed that SST, salinity, and mixed layer depth (but only as defined by the surface offset method) were weakly increasing over 1989–2016. Concomitant to geographic and physical trends, we also confirm the increase of primary production, as well as phytoplankton standing stock derived from chl *a* in the euphotic zone, throughout the data record at Station ALOHA, as previously reported by Corno et al. (2007) and Karl and Church (2017). It is unclear whether long-term trends in T chl *a* and NPP are associated with changes in nutrient inputs (Luo et al., 2012; Letelier et al., in preparation), community structure, and or increased efficiency of photosynthesis, particularly in the DCM (Letelier et al., 2017).

While lags in how climate oscillations affect *in situ* conditions at Station ALOHA relative to the rest of the gyre may suggest better agreement with respect to expanding oligotrophy, the divergence of secular trends measured by satellite-based geography and *in situ* conditions at Station ALOHA point toward an alternative hypothesis. *In situ* PP in the surface appears to be balanced by loss on diurnal time scales (White et al., 2017), allowing no accumulation of biomass through time. In our study, we found that secular trends of phytoplankton appear to be stronger in the deeper light-limited region of the euphotic zone, below the optical depth that satellites can see. Increased NPP in the DCM is correlated with greater abundances of nanophytoplankton (White et al., 2015), which represent over 40% of the particulate carbon (Barone et al., 2015). However, the debate about what exactly ^{14} C incubations measure (NPP, gross PP or something in between, e.g., Marra, 2009) is exacerbated when considering shifts in community structure, particularly toward increased dominance by nano- and picophytoplankton. Species with relatively high ratios of respiration to photosynthesis may tend to substantially overestimate net primary production, perhaps because a substantial percentage of the carbon respired by such species is old carbon (Pei and Laws, 2013). ^{14}C also overestimates NPP at low growth rates, although the discrepancy is less in 12-h than in 24-h incubations (Pei and Laws, 2014). Certainly, careful intercomparison of incubation and bottle-free

methods (e.g., Quay et al., 2010; Juranek and Quay, 2013), optical assessments of size structure (White et al., 2015) and gross carbon accumulation (White et al., 2017) along with 1-D modeling (e.g., Luo et al., 2012) will be helpful to determine how long-term changes in physical and chemical parameters are affecting the ecosystem structure and function at Station ALOHA.

Our results also suggest that long-term satellite and 3-D modeling studies, particularly those that parameterize multiple species and currencies of production (e.g., Luo et al., 2012; Nicholson et al., 2014) are necessary to understand the spatial and temporal scales of physical forcing and ecological responses in the NPSG. We note that, although the 30+ year record may be sufficient to examine many oscillations, a modeling study determined that ∼40 years was necessary to detect secular trends in the subtropics (Henson et al., 2010). However, the relationships between the geographic indicators and conditions at Station ALOHA revealed in this study may allow for future hypotheses to be tested, particularly those that relate to the role of mesoscale variability in modulating seasonal to interannual change and the role of Station ALOHA as an early indicator of gyre responses to climate oscillations.

CONCLUSION

Through the lens of pelagic seascape ecology, we have quantified different geographic systems in the North Pacific that expand and contract on seasonal and interannual scales and have embedded long-term Eulerian *in situ* observations from Station ALOHA in a dynamic mosaic of the NPSG. Over a three-decade time-series, we were able to quantify subtle secular trends and strong oscillations in gyre-scale geographic patterns and *in situ* conditions at Station ALOHA. Due to a longer data record and improved sensitivity of satellite algorithms to low-level chl *a*, we observe secular trends that are weaker than previously reported, but evident in both physical and biological definitions of the gyre, physical changes at Station ALOHA, and changes in phytoplankton standing stock and NPP, primarily in the deeper euphotic zone. Finally, we observe that conditions at Station ALOHA shift analogously to strong interannual oscillations in gyre-scale oligotrophy as defined by multivariate seascapes, with shoaled mixed layer and declines in phytoplankton biomass and production occurring with an expanded subtropical seascape.

AUTHOR CONTRIBUTIONS

MK: Devised the original question with input from CD and RL, created the study design, and analyzed the data with input from SD; MC and DK: Contributed data and historical context to the manuscript. All authors contributed to the writing and editing of the manuscript.

ACKNOWLEDGMENTS

We acknowledge support from the National Science Foundation through the Center for Microbial Oceanography: Research and Education (C-MORE), an NSF Science and Technology Center (EF-0424599), and the Hawaii Ocean Time-series (OCE-1260164; MC and DK), and the National Aeronautics and Space Administration Ocean Biology and Biogeochemistry Program (NASA NNX14AM36G, SD and MK) and the Biodiversity and Ecological Forecasting Program (NNX14AP62A and 80NSSC18K0412, MK). Additional support was provided by the Gordon and Betty Moore Foundation (#3794; DK) and the Simons Foundation's SCOPE project (#329104 ; DK).

SUPPLEMENTARY MATERIAL

The Supplementary Material for this article can be found online at: https://www.frontiersin.org/articles/10.3389/fmars.2018.00130/full#supplementary-material

Figure S1 | Seascape determination of dynamic gyre geography. **(A)** Variance explained by satellite and model seascapes and the percent of pixels that have the same classification in space and time between satellite and modeled seascapes. **(B)** Cross-correlation of model and satellite time series of subtropical seascape expansion. **(C)** Cross-correlation of model and satellite time series of isolation of Station ALOHA.

Figure S2 | Cross-correlation of MEI and PDO with NPGO.

Figure S3 | Cross-correlation of geographic indicators. **(A)** Areal extent of low level chl *a*, extent defined by geostrophy, and isolation distance of Station ALOHA in relation to variations in subtropical seascape extent. **(B)** Areal extent of low level chl *a*, extent defined by geostrophy, and subtropical seascape extent in relation to variations in the isolation distance of Station ALOHA within the subtropical seascape.

Figure S4 | Cross correlation analysis of climate indices and *in situ* surface properties at station ALOHA.

Table S1 | Trends of subtropical expansion across geographic metrics, chl *a* algorithms, and time-series duration. Italicized values denote no significant trend over the duration measured. The effect of climate oscillations has not been removed.

REFERENCES

Anouar, F., Badran, F., and Thiria, S. (1998). Probabilistic self-organizing map and radial basis function networks. *Neurocomputing* 20, 83–96. doi: 10.1016/S0925-2312(98)00026-5

Barone, B., Bidigare, R. R., Church, M.J., Karl, D.M., Letelier, R.M., and White, A.E. (2015). Particle distributions and dynamics in the euphotic zone of the North Pacific Subtropical Gyre. *J. Geophys. Res. Oceans* 120, 3229–3247. doi: 10.1002/2015JC010774

Behrenfeld, M. J., O'Malley, R. T., Boss, E. S., Westberry, T. K., Graff, J. R., Halsey, K. H., et al. (2016). Revaluating ocean warming impacts on global phytoplankton. *Nat. Clim. Chang.* 6, 323–330. doi: 10.1038/nclimate2838

Behrenfeld, M. J., O'Malley, R., T., Siegel, D. A., McClain, C. R., Sarmiento, J. L., Feldman, G. C., et al. (2006). Climate-driven trends in contemporary ocean productivity. *Nature* 444, 752–755. doi: 10.1038/nature05317

Bidigare, R. R., Benitez-Nelson, C., Leonard, C. L., Quay, P. D., Parsons, M. L., Foley, D. G., et al. (2003). Influence of a cyclonic eddy on microheterotroph biomass and carbon export in the lee of Hawaii. *Geophys. Res. Lett.* 30:1318. doi: 10.1029/2002GL01639

Boyce, D. G., Dowd, M., Lewis, M. R., and Worm, B. (2014). Estimating global chlorophyll changes over the past century. *Prog. Oceanogr.* 122, 163–173. doi: 10.1016/j.pocean.2014.01.004

Boyce, D. G., Lewis, M. R., and Worm, B. (2010). Global phytoplankton decline over the past century. *Nature*, 466, 591–596. doi: 10.1038/nature09268

Boyce, D. G., Lewis, M. R., and Worm, B. (2011). Boyce et al. reply. *Nature*, 472, E8–E9. doi: 10.1038/nature09953

Campbell, L., Liu, H., Nolla, H. A., and Vaulot, D. (1997). Annual variability of phytoplankton and bacteria in the subtropical North Pacific Ocean at Station ALOHA during the 1991–1994 ENSO event. *Deep Sea Res. Part I Oceanogr. Res. Pap.* 44, 167–192. doi: 10.1016/S0967-0637(96)00102-1

Chai, F., Jiang, M., Barber, R., Dugdale, R., and Chao, Y. (2003). Interdecadal variation of the transition zone chlorophyll front: a physical-biological model simulation between 1960 and 1990. *J. Oceanogr.* 59, 461–475. doi: 10.1023/A:1025540632491

Chavez, F. P., Messié, M., and Pennington, J. T. (2011). Marine primary production in relation to climate variability and change. *Ann. Rev. Mar. Sci.* 3, 227–260. doi: 10.1146/annurev.marine.010908.163917

Chelton, D. B., Schlax, M. G., and Samelson, R. M. (2011). Global observations of nonlinear mesoscale eddies. *Prog. Oceanogr.* 91, 167–216. doi: 10.1016/j.pocean.2011.01.002

Church, M. J., Mahaffey, C., Letelier, R. M., Lukas, R., Zehr, J. P., and Karl, D. M. (2009). Physical forcing of nitrogen fixation and diazotroph community structure in the North Pacific subtropical gyre. *Glob. Biogeochem. Cycles* 23:GB2020. doi: 10.1029/2008GB003418

Corno, G., Karl, D. M., Church, M. J., Letelier, R. M., Lukas, R., Bidigare, R. R., et al. (2007). Impact of climate forcing on ecosystem processes in the North Pacific Subtropical Gyre. *J. Geophys. Res. Oceans* 112:C04021. doi: 10.1029/2006JC003730

Di Lorenzo, E., Schneider, N., Cobb, K., M., Franks, P. J. S., Chhak, K., Miller, A. J., et al. (2008). North Pacific Gyre Oscillation links ocean climate and ecosystem change. *Geophys. Res. Lett.* 35:L08607. doi: 10.1029/2007GL032838

Di Lorenzo, E., Fiechter, J., Schneider, N., Bracco, A., Miller, A. J., Franks, P. J. S., et al., (2009). Nutrient and salinity decadal variations in the central and eastern North Pacific. *Geophys. Res. Lett.* 36:L14601. doi: 10.1029/2009GL038261

DiTullio, G. R., and Laws, E. A. (1991). Impact of an atmospheric-oceanic disturbance on phytoplankton community dynamics in the North Pacific Central Gyre. *Deep Sea Res. Part A Oceanogr. Res. Pap.* 38, 1305–1329. doi: 10.1016/0198-0149(91)90029-F

Doney, S. C., Lima, I., Feely, R. A., Glover, D. M., Lindsay, K., Mahowald, N., et al. (2009). Mechanisms governing interannual variability in upper-ocean inorganic carbon system and air–sea CO_2 fluxes: physical climate and atmospheric dust. *Deep Sea Res. Part II Top. Stud. Oceanogr.* 56, 640–655. doi: 10.1016/j.dsr2.2008.12.006

Dore, J. E., Lukas, R., Sadler, D. W., Church, M. J., and Karl, D. M. (2009). Physical and biogeochemical modulation of ocean acidification in the central North Pacific. *Proc. Natl. Acad. Sci. U.S.A.* 106, 12235–12240. doi: 10.1073/pnas.0906044106

Emerson, S., Quay, P., Karl, D., Winn, C., Tupas, L., and Landry, M. (1997). Experimental determination of the organic carbon flux from open-ocean surface waters. *Nature* 389, 951–954. doi: 10.1038/40111

Fong, A. A., Karl, D. M., Lukas, R., Letelier, R. M., Zehr, J. P., and Church, M. J. (2008). Nitrogen fixation in an anticyclonic eddy in the oligotrophic North Pacific Ocean. *ISME J.* 2, 663–676. doi: 10.1038/ismej.2008.22

Franz, B. A. (2009). *Methods for Assessing the Quality and Consistency of Ocean Color Products.* NASA Goddard Space Flight Center, Ocean Biology Processing Group. Available online at: https://oceancolor.gsfc.nasa.gov/docs/methods/sensor_analysis_methods/

Franz, B. A., Bailey, S. W., Werdell, P. J., and McClain, C. R. (2007). Sensor-independent approach to the vicarious calibration of satellite ocean color radiometry. *Appl. Opt.* 46:5068. doi: 10.1364/AO.46.005068

Gille, S. T. (2014). Meridional displacement of the Antarctic Circumpolar Current. *Phil. Trans. R. Soc. A* 372:20130273. doi: 10.1098/rsta.2013.0273

Glover, D.M., Jenkins, W.J., and Doney, S.C. (2011). *Modeling Methods for Marine Science*. Cambridge: Cambridge University Press.

Guidi, L., Calil, P. H., Duhamel, S., Björkman, K. M., Doney, S. C., Jackson, G. A., et al. (2012). Does eddy-eddy interaction control surface phytoplankton distribution and carbon export in the North Pacific Subtropical Gyre? *J. Geophys. Res.* 117:G02024. doi: 10.1029/2012JG001984

Hammond, M. L., Beaulieu, C., Sahu, S. K., and Henson, S. A. (2017), Assessing trends and uncertainties in satellite-era ocean chlorophyll using space-time modeling. *Glob. Biogeochem. Cycles* 31, 1103–1117. doi: 10.1002/2016GB005600

Henson, S. A., Sarmiento, J. L., Dunne, J. P., Bopp, L., Lima, I., Doney, S. C., et al. (2010). Detection of anthropogenic climate change in satellite records of ocean chlorophyll and productivity. *Biogeosciences* 7, 621–640. doi: 10.5194/bg-7-621-2010

Hu, C., Lee, Z., and Franz, B. (2012). Chlorophyll a algorithms for oligotrophic oceans: a novel approach based on three-band reflectance difference. *J. Geophys. Res. Oceans* 117:C01011. doi: 10.1029/2011JC007395

Irwin, A. J., and Oliver, M. J. (2009). Are ocean deserts getting larger? *Geophys. Res. Lett.* 36:L18609. doi: 10.1029/2009GL039883

Juranek, L. W., and Quay, P. D. (2013). Using triple isotopes of dissolved oxygen to evaluate global marine productivity. *Ann. Rev. Mar. Sci.* 5, 503–524. doi: 10.1146/annurev-marine-121211-172430

Karl, D. M. (2010). Oceanic ecosystem time-series programs: ten lessons learned. *Oceanography* 23, 104–125. doi: 10.5670/oceanog.2010.27

Karl, D. M., Bidigare, R. R., and Letelier, R. M. (2001). Long-term changes in plankton community structure and productivity in the North Pacific Subtropical Gyre: the domain shift hypothesis. *Deep Sea Res. Part II Top. Stud. Oceanogr.* 48, 1449–1470. doi: 10.1016/S0967-0645(00)00149-1

Karl, D. M., and Church, M. J. (2017). Ecosystem structure and dynamics in the North Pacific Subtropical Gyre: new views of an old ocean. *Ecosystems* 20, 433–457. doi: 10.1007/s10021-017-0117-0

Karl, D. M., Letelier, R., Hebel, D., Tupas, L., Dore, J., Christian, J., et al. (1995). Ecosystem changes in the North Pacific subtropical gyre attributed to the 1991-92 El Niño. *Nature* 373, 230–234. doi: 10.1038/373230a0

Karl, D. M., and Lukas, R. (1996). The Hawaii Ocean Time-series (HOT) program: background, rationale and field implementation. *Deep Sea Res. Part II Top. Stud. Oceanogr.* 43, 129–156. doi: 10.1016/0967-0645(96)00005-7

Kavanaugh, M.T., Emerson, S. R., Lockwood, D. M., Quay, P.D., and Letelier, R. M. (2014a). Physicochemical and biological controls on primary and net community production across NE Pacific seascapes. *Limnol. Oceanogr.* 59, 2013–2027. doi: 10.4319/lo.2014.59.6.2013

Kavanaugh, M. T., Hales, B., Saraceno, M., Spitz, Y. H., White, A. E., and Letelier, R. M. (2014b). Hierarchical and dynamic seascapes: a quantitative framework for scaling pelagic biogeochemistry and ecology. *Prog. Oceanogr.* 120, 291–304. doi: 10.1016/j.pocean.2013.10.013

Kavanaugh, M. T., Oliver, M., Chavez, F., Letelier, R. M., Muller-Karger, F., and Doney, S. C. (2016). Seascapes as a new vernacular for ocean monitoring, management and conservation. *ICES J. Mar. Sci.* 73, 1839–1850. doi: 10.1093/icesjms/fsw086

Letelier, R. M., Bidigare, R. R., Hebel, D. V., Ondrusek, M., Winn, C. D., and Karl, D. M. (1993). Temporal variability of phytoplankton community structure based on pigment analysis. *Limnol. Oceanogr.* 38, 1420–1437. doi: 10.4319/lo.1993.38.7.1420

Letelier, R. M., Dore, J. E., Winn, C. D., and Karl, D. M. (1996). Seasonal and interannual variations in photosynthetic carbon assimilation at Station ALOHA. *Deep Sea Res. Part II Top. Stud. Oceanogr.* 43, 467–490. doi: 10.1016/0967-0645(96)00006-9

Letelier, R. M., Karl, D. M., Abbott, M. R., Flament, P., Freilich, M., Lukas, R., et al. (2000). Role of late winter mesoscale events in the biogeochemical variability of the upper water column of the North Pacific Subtropical Gyre. *J. Geophys. Res. Oceans* 105, 28723–28739. doi: 10.1029/1999JC000306

Letelier, R. M., White, A. E., Bidigare, R. R., Barone, B., Church, M. J., and Karl, D. M. (2017). Light absorption by phytoplankton in the North Pacific Subtropical Gyre. *Limnol. Oceanogr.*62, 1526–1540. doi: 10.1002/lno.10515

Levitus, S., Antonov, J. I., Boyer, T. P., Baranova, O. K., Garcia, H. E., Locarnini, R. A., et al. (2012). World ocean heat content and thermosteric sea level change (0–2000 m), 1955–2010. *Geophys. Res. Lett.* 39:L10603. doi: 10.1029/2012GL051106

Li, B., Karl, D. M., Letelier, R. M., and Church, M. J. (2011). Size-dependent photosynthetic variability in the North Pacific Subtropical Gyre. *Mar. Ecol. Prog. Ser.* 440, 27–40. doi: 10.3354/meps09345

Lomas, M. W., Steinberg, D. K., Dickey, T., Carlson, C. A., Nelson, N. B., Condon, R. H., et al. (2010). Increased ocean carbon export in the Sargasso Sea linked to climate variability is countered by its enhanced mesopelagic attenuation. *Biogeosciences* 7, 57–70, doi: 10.5194/bg-7-57-2010

Luo, Y.-W., Ducklow, H. W., Friedrichs, M. A. M., Church, M. J. Karl, D. M., and Doney, S. C. (2012). Interannual variability of primary production and

dissolved organic nitrogen storage in the North Pacific Subtropical Gyre. *J. Geophys Res.* 117:G03019. doi: 10.1029/2011JG001830

Mantua, N. J., Hare, S. R., Zhang, Y., Wallace, J. M., and Francis, R. C. (1997). A Pacific interdecadal climate oscillation with impacts on salmon production. *Bull. Am. Meteorol. Soc.* 78, 1069–1079. doi: 10.1175/1520-0477(1997)078<1069:APICOW>2.0.CO;2

Marra, J. (2009). Net and gross productivity: weighing in with ^{14}C. *Aquat. Microbial. Ecol.* 56, 123–131. doi: 10.3354/ame01306

Martin, J. H., Knauer, G. A., Karl, D. M., and Broenkow, W.W. (1987). VERTEX: carbon cycling in the northeast Pacific. *Deep Sea Res. Part A Oceanogr. Res. Pap.* 34, 267–285. doi: 10.1016/0198-0149(87)90086-0

McCune, B., Grace, J. B., and Urban, D. L. (2002). *Analysis of Ecological Communities Vol. 28*. Gleneden Beach, OR: MjM software design.

McQuatters-Gollop, A., Reid, P. C., Edwards, M., Burkill, P. H., Castellani, C., Batten, S., et al. (2011). Is there a decline in marine phytoplankton? *Nature* 472, E6–E7. doi: 10.1038/nature09950

Messié, M. and Chavez, F. P. (2011). Global modes of sea surface temperature variability in relation to regional climate indices. *J. Climate* 24, 4313–4330. doi: 10.1175/2011JCLI3941.1

Moore, J. K., Lindsay, K., Doney, S. C., Long, M. C., and Misumi, K. (2013). Marine ecosystem dynamics and biogeochemical cycling in the Community Earth System Model CESM1(BGC). *Clim. J.* 26, 9291–9321. doi: 10.1175/JCLI-D-12-00566.1

Nicholson, D., Stanley, R. H. and Doney, S. C. (2014). The triple oxygen isotope tracer of primary productivity in a dynamic ocean model. *Glob. Biogeochem. Cycles* 28, 538–552. doi: 10.1002/2013GB004704

Oliver, M. J., and Irwin, A. J. (2008). Objective global ocean biogeographic provinces. *Geophys. Res. Lett.* 35:L15601. doi: 10.1029/2008GL034238

Pei, S., and Laws, E. A. (2013). Does the ^{14}C method estimate net photosynthesis? Implications from batch and continuous culture studies of marine phytoplankton. *Deep Sea Res. Part I Oceanogr. Res. Pap.* 82, 1–9. doi: 10.1016/j.dsr.2013.07.011

Pei, S., and Laws, E. A. (2014). Does the ^{14}C method estimate net photosynthesis? II. Implications from cyclostat studies of marine phytoplankton. *Deep Sea Res. Part I Oceanogr. Res. Pap.* 91, 94–100. doi: 10.1016/j.dsr.2014.05.015

Polovina, J. J., Howell, E. A., and Abecassis, M. (2008). Ocean's least productive waters are expanding. *Geophys. Res. Lett.* 35:L03618. doi: 10.1029/2007GL031745

Quay, P. D., Peacock, C., Björkman, K., and Karl, D. M. (2010). Measuring primary production rates in the ocean: Enigmatic results between incubation and non-incubation methods at Station ALOHA, Global Biogeochem. *Cycles* 24:GB3014. doi: 10.1029/2009GB003665

Saba, V. S., Friedrichs, M. A. M., Carr, M.-E., Antoine, D., Armstrong, R. A., Asanuma, I., (2010). Challenges of modeling depth-integrated marine primary productivity over multiple decades : a case study at BATS and HOT. *Glob. Biogeochem. Cycles*. 24:GB3020. doi: 10.1029/2009GB003655

Sakamoto, C. M., Karl, D. M., Jannasch, H. W., Bidigare, R. R., Letelier, R. M., Walz, P. M., et al. (2004). Influence of Rossby waves on nutrient dynamics and the plankton community structure in the North Pacific subtropical gyre. *J. Geophys. Res. Oceans* 109:C05032. doi: 10.1029/2003JC001976

Siegel, D.A., Behrenfeld, M. J., Maritorena, S., McClain, C. R., Antoine, D., Bailey, S. W., et al. (2013). Regional to global assessments of phytoplankton dynamics from the SeaWiFS mission. *Remote Sens. Environ.* 135, 77–91. doi: 10.1016/j.rse.2013.03.025

Signorini, S. R., Franz, B. A., and McClain, C. R. (2015). Chlorophyll variability in the oligotrophic gyres: mechanisms, seasonality and trends. *Front. Mar. Sci.* 2:1. doi: 10.3389/fmars.2015.00001

Signorini, S. R., and McClain, C. R. (2012). Subtropical gyre variability as seen from satellites. *Remote Sens. Lett.* 3, 471–479. doi: 10.1080/01431161.2011.625053

Sverdrup, H. U., Johnson, M. W., and Fleming, R. H. (1942). *The Oceans, Their Physics, Chemistry, and General Biology. Vol. 1087*. New York, NY: Prentice-Hall.

Vaillancourt, R. D., Marra, J., Seki, M. P., Parsons, M. L., and Bidigare, R. R. (2003). Impact of a cyclonic eddy on phytoplankton community structure and photosynthetic competency in the subtropical North Pacific Ocean. *Deep Sea Res. Part I Oceanogr. Res. Pap.* 50, 829–847. doi: 10.1016/S0967-0637(03)00059-1

Venrick, E. L. (1995). "Scales of variability in a stable environment: phytoplankton in the central North Pacific," in *Ecological Time Series*. eds T. M. Powell and J. H. Steele(Boston, MA: Springer).

Venrick, E. L., McGowan, J. A., Cayan, D. R., and Hayward, T. L. (1987). Climate and chlorophyll a: long-term trends in the central North Pacific Ocean. *Science* 238, 70–72. doi: 10.1126/science.238.4823.70

Ward, J. (1963). Hierarchical grouping to optimize an objective function. *J. Am. Stat. Assoc.* 58, 236–244. doi: 10.1080/01621459.1963.10500845

White, A. E., Barone, B., Letelier, R. M., and Karl, D. M. (2017). Productivity diagnosed from the diel cycle of particulate carbon in the North Pacific Subtropical Gyre. *Geophys. Res. Lett.* 44, 3752–3760. doi: 10.1002/2016GL071607

White, A. E., Letelier, R. M., Whitmire, A. L., Barone, B., Bidigare, R. R., Church, M. J., et al. (2015). Phenology of particle size distributions and primary productivity in the North Pacific subtropical gyre (Station ALOHA). *J. Geophys. Res. Oceans* 120, 7381–7399. doi: 10.1002/2015JC010897

Wilson, C., and Adamec, D. (2001). Correlations between surface chlorophyll and sea surface height in the tropical Pacific during the 1997–1999 El Niño-Southern Oscillation event. *J. Geophys. Res. Oceans* 106, 31175–31188. doi: 10.1029/2000JC000724

Winn, C. D., Campbell, L., Christian, J. R., Letelier, R. M., Hebel, D. V., Dore, J. E., et al. (1993). Seasonal variability in the phytoplankton community of the North Pacific Subtropical Gyre. *Glob. Biogeochem. Cycles* 9, 605–620. doi: 10.1029/95GB02149

Wright, S. W., Jeffrey, S. W., Mantoura, R. F. C., Llewellyn, C. A., Bjørnland, T., and Repeta, D. (1991). Improved HPLC method for the analysis of chlorophylls and carotenoids from marine phytoplankton. *Mar. Ecol. Prog. Ser.* 77, 183–196.

Wolter, K., and Timlin, M. S. (1993). "Monitoring ENSO in COADS with a seasonally adjusted principal component index," in *Proceedings of the17th Climate Diagnostics Workshop*, Vol. 5257 (Norman, OK).

Zhang, Y., Wallace, J. M., and Battisti, D. S. (1997). ENSO-like interdecadal variability: 1900–93. *J. Clim.* 10, 1004–1020. doi: 10.1175/1520-0442(1997)010<1004:ELIV>2.0.CO;2

Conflict of Interest Statement: The authors declare that the research was conducted in the absence of any commercial or financial relationships that could be construed as a potential conflict of interest.